

**MELTING IN THE DEEP LUNAR MANTLE.** C.K. Shearer<sup>1</sup>, C. Neal<sup>2</sup>, D. Draper<sup>1</sup>, J.J. Papike<sup>1</sup> and C. Agee<sup>1</sup>. <sup>1</sup>Institute of Meteoritics, Department of Earth and Planetary Sciences, MSC03-2050, 1 University of New Mexico, Albuquerque, New Mexico, 87131-0001. <sup>2</sup> Dept. Civil Eng. & Geological Sciences, University of Notre Dame, Notre Dame, IN 46556. (cshearer@unm.edu)

**Introduction:** Whereas previous experimental studies [1,2,3] and interpretation of Apollo seismic experiments [4,5] are permissive for garnet in the deep lunar mantle, interpretations of Lu-Hf isotopic systematics [6] and trace element data [7] seem to require garnet in the source of selected mare basalts. Understanding the mineralogy of the deep lunar mantle is critical to our further interpretation of the structure of the Moon and modeling early lunar differentiation. Also, as it has been suggested that some mare basalts may be the product of melting that was initiated at depths to 1000 km, the stability of phases such as garnet may affect basalt composition and magma transport. To better understand melting in the deep lunar mantle we have initiated a study that focuses upon both the trace element characteristics of mare basalts and pyroclastic glasses and the high pressure (> 2.5 GPa) phase equilibria of pyroclastic glass compositions. Here we report the initial high pressure results on picritic glass compositions and ion probe trace element study of the pyroclastic glasses with an emphasis on elements that could potentially be fractionated by garnet. In addition to continuing this line of experiments, an additional facet of this study will focus upon a comparison of trace elements between mare basalts and pyroclastic glasses using comparable ion probe-ICP-MS data sets.

**Analytical Approach:** For this study, we initially started with the Apollo 15 and 17 pyroclastic glasses. Prior to trace element analysis, individual glasses were imaged and analyzed using a JEOL 733 superprobe. Selected trace elements (<sup>45</sup>Sc, <sup>89</sup>Y, <sup>90</sup>Zr, <sup>140</sup>Ce, <sup>174</sup>Yb, <sup>176</sup>Hf, <sup>180</sup>Hf) that would be useful in evaluating the presence of garnet in the source were measured using the Cameca ims 4f operated on the University of New Mexico campus by IOM. Analyses were made using primary O<sup>-</sup> ions accelerated through a nominal potential of 10.0 kV. A primary beam current of 20 nA was focused on the sample over a spot diameter of 20 μm. Sputtered secondary ions were energy filtered using a sample offset voltage of 105 V and an energy window of ± 25 V. Analyses involved repeated cycles of peak counting. The analytical procedure included counting on a background position to monitor detection noise. Absolute concentrations of each element were calculated using empirical relationships of Trace Element<sup>+</sup>/<sup>30</sup>Si<sup>+</sup> ratios (normalized to known SiO<sub>2</sub> content) to element concentrations as derived from daily calibration. Calibration curve was constructed using multiple

glass standards (> 3) for each element. Calibration curves for each element have correlation coefficients of greater than 0.97. Average values for Hf for the green and orange glasses as determined by ion probe are 0.63 and 7.3 ppm, respectively. The average values for Hf for bulk Apollo 15 green and Apollo 17 orange glasses are 0.6 and 5.8 ppm, respectively. All analyses are referenced to a single basalt glass standard that will then be used as a comparative reference to future ICP-MS analysis of crystalline mare basalts.

**Experimental Approach:** High pressure experiments are being carried out in the IOM high pressure experimental lab at pressures between 2.0 and 4.5 GPa using synthetic Apollo 15 green C glass and Apollo 14 black glass compositions. These compositions span nearly the entire range of lunar pristine glasses, and these pressures range to the deepest parts of the lunar mantle.

#### Results:

**High Pressure Experiments.** Apollo 15 green glass C is saturated with garnet and clinopyroxene at 4.5 GPa and 1775°C (Fig. 1). Additional experiments will determine which phase is on the liquidus.

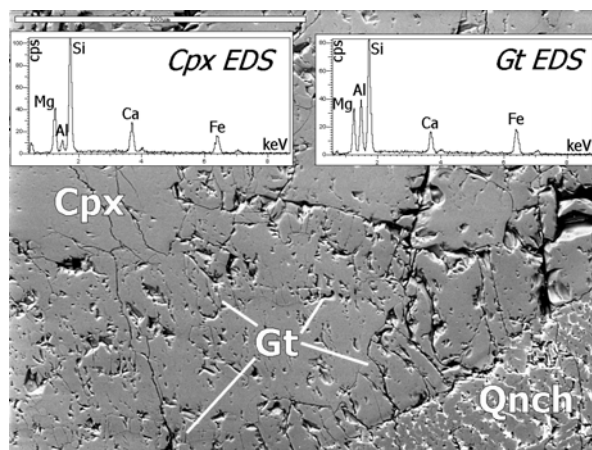


**Figure 1.** Run A4, A-15 green C at 4.5 GPa, 1775°C. Cpx, clinopyroxene; Gt, garnet; Qnch, quenched melt.

**Ion Microprobe Analyses of the Pyroclastic Glasses.** The Apollo 15 green glasses possibly represent near-primary, very low-TiO<sub>2</sub> basalts (≈0.2 to 0.7 wt.% TiO<sub>2</sub>) with Mg# as high as 0.68. The REE patterns of the Apollo 15 green glasses are relatively flat to slightly LREE depleted with small negative Eu anomalies and REE abundances between 2 and 8 times chondrite. Ni and Co range from 90-200 ppm and 40-

70 ppm, respectively [8,9]. Individual green glass spheres have been classified into 5 distinct geochemical groups (A-E) [10]. Our new high precision ion probe analyses indicate that compared to the other Apollo 15 green glasses, the group C glasses are higher in overall incompatible element concentrations,  $[Yb/Ce]_N$ ,  $[Sc/Yb]_N$ , and  $[Yb/Hf]_N$ . There appears to be limited correlation among these ratios among all the Apollo 15 green glasses.

The Apollo 14 green glasses also represent near-primary, very low- $TiO_2$  basalts ( $\approx 0.6$  to  $1.3$  wt.%  $TiO_2$ ) with Mg# as high as 0.63. Their trace element characteristics are distinct from those of the Apollo 15 green glass. The REE patterns of the Apollo 14 green glasses are generally LREE enriched with small to moderate negative Eu anomalies and REE abundances between 10 and 70 times chondrite. Ni and Co range from 160-200 ppm and 60-70 ppm, respectively [8,9]. Individual green glass spheres have been classified into 4 distinct geochemical groups (VLT, A, B1, B2) [9,10]. Compared to the Apollo 15 green glass, the Apollo 14 green glass is enriched in Hf (3 to 6 ppm) and has lower  $[Yb/Ce]_N$ ,  $[Sc/Yb]_N$ , and  $[Yb/Hf]_N$ .

The Apollo 17 orange glasses possibly represent near-primary high- $TiO_2$  basalts ( $\approx 8.4$  to  $9.4$  wt.%  $TiO_2$ ) with Mg# as high as 0.54. The REE patterns of the Apollo 17 orange glasses are concave downward with slightly larger negative Eu anomalies and REE abundances between 20 and 60 times chondrite. Ni and Co range from 30-70 ppm and 48-65 ppm, respectively [8,9]. Individual orange glass spheres have been classified into 3 distinct geochemical groups [10]. Compared to the Apollo 15 green glass, the orange glass has lower  $[Sc/Yb]_N$ ,  $[Hf/Yb]_N$ , and  $[Ce/Yb]_N$ . Based on the small population that we have analyzed, there appears to be no systematic variations in these elements among the different types of Apollo 17 orange glass

**Discussion:** Previous experiments on several high- and low-Ti mare basalts indicate that garnet and pyroxene ( $\pm$  spinel) are in equilibrium with melt at pressures between 1.8 and 2.5 GPa [1,2,3]. Under these conditions, pyroxene is the sole liquidus phase. Our initial high pressure experiments show that garnet coexists with calcic pyroxene and melt at 4.5 GPa for Apollo 15 green C glass compositions. Thus far our experiments do not demonstrate whether garnet is consumed during melting prior to that of the coexisting pyroxene. How the composition of the garnets influence the partitioning behavior of trace elements during melting will be further explored.

The initial trace element data we have collected on some of the pyroclastic glasses hint at the possibility

that garnet may have been involved in their petrogenesis. The Apollo 15 green C glasses exhibit more extensive fractionation of Ce and Hf from Yb than do the other Apollo 15 green glasses. This could be interpreted as indicating that garnet played a more important role during melting. For example, the melting that produced green C may have occurred in the garnet stability field and consumed garnet. Alternatively, if melting was initiated in the garnet stability field and continued outside the garnet stability field the garnet signature in the Apollo 15 green C melt may reflect the relative extent of melting in each stability field.

The differences in incompatible elements between Apollo 14 and 15 very low-Ti glasses has been attributed to the role of KREEP [8,9]. The Apollo 14 very low-Ti glasses represent basalts that either assimilated KREEP in a shallow mantle environment or incorporated the KREEP signature during melting. An interesting aspect of our analyses is that the  $[Hf/Yb]_N$  for the Apollo 14 very-low Ti glasses ( $< 0.8$ ) is lower than both the Apollo 15 green glasses ( $> 1.6$ ) and KREEP (0.9)

How relevant is garnet to lunar magma ocean crystallization and mare basaltic magmatism? Based on compositions predicted for the lunar magma ocean and the extensive plagioclase-rich primordial crust, it appears to be unlikely that garnet would be an early precipitating phase. Neal [7] suggested that garnet was a stable phase in "primitive" lunar material that did not participate in early lunar differentiation resulting from formation of the lunar magma ocean. Alternatively, garnet could be a stable phase in "fertile" LMO cumulates that were transported into the garnet stability field by cumulate overturn.

The combined major-trace element – high pressure experimental approach as outlined here and conducted in so many previous petrologic studies of lunar magmatism is critical to understanding the deep lunar mantle and lunar magmatism. Application of such an approach to understanding the asymmetrical internal structure of the Moon by sampling other lunar terrains requires small sample volume consistent with robotic sample return missions.

**References:** [1] Longhi et al. (1974) Proc. 5th LPSC 447-469. [2] Walker et al. (1976) GSA Bull. 87, 646-656. [3] Longhi (1992) GCA 56, 2235-2251. [4] Anderson (1975) JGR 80, 1555-1557. [5] Hood and Jones (1987) Proc. 17th LPSC E396-E410. [6] Beard et al. (1998) GCA 62, 525-544. [7] Neal (2001) JGR 106, 27865-27885. [8] Shearer and Papike (1993) GCA 57, 4785-4812. [9] Shearer and Papike (1999) Am. Mineral. 84, 1469-1494. [10] Delano (1986) Proc. 16<sup>th</sup> LPSC, D201-D213.